Simulation of photon attenuation coefficients for high effective shielding material Lead-Boron Polyethyene

L Zhang, M C Jia, J J Gong, W M Xia

Department of Nuclear Science and Engineering，Naval University of Engineering，Wuhan 430033，China

E-mail: 1761276990@qq.com

Aastract. The mass attenuation coefficient of various Lead-Boron Polyethylene samples which can be used as the photon shielding materials in marine reactor, have been simulated using the MCNP-5 code, and compared with the theoretical values at the photon energy range 0.001MeV—20MeV. A good agreement has been observed. The variations of mass attenuation coefficient, linear attenuation coefficient and mean free path with photon energy between 0.001MeV to 100MeV have been plotted. The result shows that all the coefficients strongly depends on the photon energy, material atomic composition and density. The dose transmission factors for source Cesium-137 and Cobalt-60 have been worked out and their variations with the thickness of various sample materials have also been plotted. The variations show that with the increase of materials thickness the dose transmission factors decrease continuously. The results of this paper can provide some reference for the use of the high effective shielding material Lead-Boron Polyethyene.

1. Introduction

Due to the space limitations of marine reactor, their weight and volume should be as small as possible. Meanwhile, the weight and volume of shielding materials occupy a large proportion of that of reactor plant [1]. Therefore, it is important to reduce the weight and volume of the shielding materials in order to make the marine reactor lightweight and compact. The use of high effective shielding materials is an important means to achieve this goal [2]. Lead-Boron Polyethylene (PbBPE) which is formed by diffusing the boron carbide powder and lead powder in the polyethylene is one of the high effective shielding materials [3-5]. The polyethylene has good neutron shielding capability because of its high hydrogen content, boron could absorb the thermal neutrons and lead has an excellent photon shielding capability.

Accurate values of photon attenuation coefficients of shielding materials are of great significance for its engineering applications and academic research [6]. In recent years, the photon attenuation coefficients of various shielding materials such as concrete [7-10], alloy [11] and glass [12] have been studied.

MCNP is a general-purpose Monte Carlo N–Particle code that can be used for neutron, photon, electron, or coupled neutron/photon/electron transport. This code can be used to simulate the photon attenuation coefficients of shielding materials。

The aim of this paper is to determine mass attenuation coefficient (μ_m), linear attenuation coefficient (μ), mean free path (MFP) as well as dose transmission factor (DTF) of the high effective

shielding material Lead-Boron Polyethyene by the MCNP code and consequently provide some reference for the use of the Lead-Boron Polyethyene as shielding materials.

2. Materials and methods

2.1. Materials specification of PbBPE

In this study, the PbBPE samples contain polyethylene (PE) and lead (Pb) as major weight fraction contributions. The specific compositions and density of each PbBPE samples are shown in Table 1. First four samples contain PE as a dominant contributor, while Pb is the predominant component in the rest samples. The atomic percentage of PbBPE samples is calculated from the component percentage of each sample multiplies the atomic percentage of each component. The atomic percentage of each PbBPE sample is introduced to the MCNP code by the material card.

Table 1. Percentage of atomic composition of samples

Element	Samples						
	B201 0.96g/cm^3	B202 1.00g/cm^3	B203 1.10g/cm^3	P202 1.25g/cm^3	P204 1.65g/cm^3	P206 2.94g/cm^3	PB202 3.42g/cm^3
H	13.57	12.86	11.43	10.00	7.14	3.36	2.71
B	3.91	7.83	15.65				0.78
C	82.52	79.32	72.92	60.00	42.86	20.14	16.50
Pb				30.00	50.00	76.50	80.00

2.2. Geometry system

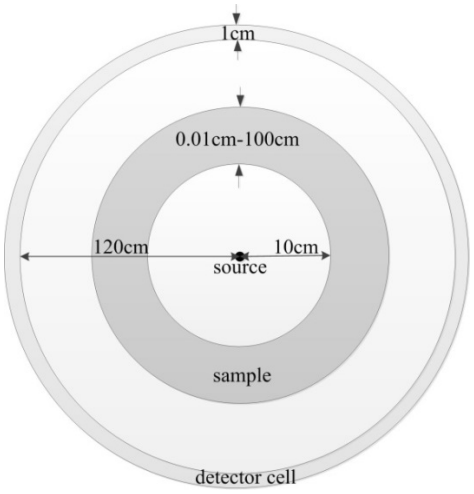

Fig.1. Schematic arrangement of MCNP simulation model

Monte Carlo N-Particle Transport (MCNP) code version 5 which uses continuous-energy nuclear and atomic data libraries was used for the simulation. The cross-sectional view of geometric model is shown in Fig 1. Its source is an isotropic point source whose particle type, energy, position and direction are defined by PAR, ERG, POS, DIR and VEC data card respectively. The sample whose thickness can be adjusted among the range of 0.01cm-100cm according to the need of the simulation is 10cm far from the source. The detector cell is 120cm far from the source and of 1cm thickness. Sample and detector cell are defined by MCNP surface and cell card.

2.3. Tally definition

Tally card F4 and tally energy (En) card was used to record the MCNP-5 simulation data when simulating the value of μ_m, μ, and *MFP*. When the *DTF* was simulated, tally card F2 as well as dose energy (DEn) card and dose function (DFn) card were used. Depending on the thickness of the sample

and the photon energy, the simulation histories as well as the variance reduction technique will change to ensure that all the simulation data passes all 10 statistical checks and the relative error is less than 1%.

2.4. Mass and linear attenuation coefficient, mean free path, dose transmission factor

The mass attenuation coefficient, linear attenuation coefficient, mean free path and dose transmission factor are simulated.

The intensity of the photons that penetrate the target without having a collision is：

$$N = N_0 e^{-\mu t} \tag{1}$$

Where N_0 (particles/cm^2) and N (particles/cm^2) are the average particle flux of Narrow beam photon in front of and behind the sample, μ (cm^{-1}) is linear attenuation coefficient in the target, t (cm) is the thickness of the sample.

Transforming equation (1), μ can be expressed as:

$$\mu = \frac{\ln \frac{N_0}{N}}{t} \tag{2}$$

The μ value is a parameter which is dependent upon density of the target, atomic number of the elements and energy of incident photon.

Mass attenuation coefficient is defined as following:

$$\mu_m = \frac{\mu}{\rho} \tag{3}$$

For mixtures and compounds, the mass attenuation coefficient can be calculated by the following equation:

$$\mu_m = \sum_{i=1}^{n} (\mu_m)_i \omega_i \qquad i = 1,2,3 \ldots n \tag{4}$$

Where $(\mu_m)_i$ and ω_i are the mass attenuation coefficient and weight percentage of the ith element in the material respectively.

The average distance that a photon moves between collisions is called the mean free path. It can be defined as:

$$MFP = \frac{1}{\mu} \tag{5}$$

The dose transmission factor which can expresses the shielding effect can be defined as:

$$DTF = \frac{H}{H_0} \tag{6}$$

Where H_0 (Sv) and N (Sv) are photon dose in front of and behind the sample. The smaller the *DTF*, the better the shielding effect.

3. Results and discussion

3.1. Mass attenuation coefficient (μ_m)

The mass attenuation coefficient values from theory based on Eq. (4) as well as those from MCNP simulation of the seven PbBPE samples for photons of energy range from 0.001MeV to 20MeV have been shown in Table 2. From this table, it can be seen that the theoretical and MCNP values are in good agreement across most energy points, only individual points have a certain difference because the use of different cross-section library.

Table 2. The theoretical and MCNP value of μ_m for different samples

Photon energy(MeV)	P202		P204		P206		PB202		B201		B202		B203	
	Theory	MCNP	Theory	MCNP	Theory	MCNP	Theory	MCNP	Theory	MCNP	Theory	MCNP	Theory	MCNP
1.00E-03	2890	3185	3553	4057	4431	5209	4543	5361	1873	1856	1851	1831	1805	1782
1.50E-03	1127	1173	1478	1552	1943	2055	2003	2123	592.8	598.3	585.1	590.0	569.8	574.0
2.00E-03	567.2	574.7	772.3	783.6	1044	1062	1079	1100	256.1	258.6	252.6	254.9	245.8	247.9
3.00E-03	643.8	597.6	1021	945.6	1521	1409	1587	1472	76.44	76.11	75.37	75.00	73.24	72.71
4.00E-03	398.0	443.8	641.7	719.4	964.6	1085	1007	1135	31.99	31.03	31.53	30.57	30.62	29.68
5.00E-03	230.6	246.3	373.4	400.9	562.6	606.0	587.6	633.8	16.21	15.33	15.98	15.09	15.51	14.64
6.00E-03	146.8	152.0	238.3	248.3	359.6	376.3	375.6	393.8	9.307	8.613	9.171	8.477	8.898	8.216
8.00E-03	71.39	71.15	116.3	116.5	175.9	177.4	183.7	185.8	3.921	3.484	3.863	3.426	3.749	3.322
1.00E-02	40.64	40.04	66.34	65.85	100.4	100.4	104.9	105.1	2.060	1.805	2.030	1.778	1.971	1.725
1.50E-02	34.00	33.36	56.17	55.41	85.55	84.86	89.43	88.90	0.736	0.621	0.726	0.612	0.707	0.596
2.00E-02	26.21	25.40	43.40	42.25	66.17	64.70	69.17	67.79	0.427	0.356	0.422	0.352	0.412	0.343
3.00E-02	9.285	8.779	15.30	14.55	23.26	22.33	24.31	23.45	0.268	0.234	0.265	0.231	0.260	0.227
4.00E-02	4.467	4.161	7.294	6.846	11.04	10.30	11.53	10.80	0.225	0.205	0.223	0.203	0.219	0.199
5.00E-02	2.558	2.330	4.125	3.780	6.200	5.760	6.474	6.049	0.206	0.193	0.205	0.191	0.201	0.188
6.00E-02	1.644	1.477	2.609	2.356	3.887	3.557	4.056	3.709	0.195	0.186	0.193	0.184	0.190	0.181
8.00E-02	0.853	0.748	1.301	1.139	1.893	1.676	1.971	1.746	0.181	0.175	0.179	0.174	0.176	0.170
1.00E-01	1.785	1.713	2.860	2.734	4.285	4.122	4.473	4.333	0.170	0.167	0.169	0.165	0.166	0.162
1.50E-01	0.712	0.677	1.084	1.034	1.577	1.503	1.642	1.571	0.152	0.150	0.151	0.149	0.148	0.146
2.00E-01	0.398	0.378	0.569	0.540	0.797	0.753	0.827	0.779	0.139	0.138	0.138	0.137	0.135	0.134
3.00E-01	0.206	0.196	0.262	0.247	0.337	0.314	0.347	0.323	0.120	0.120	0.119	0.119	0.117	0.117
4.00E-01	0.146	0.140	0.171	0.161	0.203	0.189	0.207	0.192	0.108	0.108	0.107	0.107	0.105	0.105
5.00E-01	0.118	0.114	0.130	0.124	0.147	0.137	0.149	0.138	0.099	0.098	0.098	0.097	0.096	0.096
6.00E-01	0.102	0.099	0.108	0.103	0.117	0.110	0.118	0.110	0.091	0.091	0.090	0.090	0.089	0.088
8.00E-01	0.083	0.081	0.085	0.082	0.087	0.082	0.087	0.082	0.080	0.080	0.079	0.079	0.078	0.078
1.00E+00	0.072	0.071	0.072	0.070	0.071	0.069	0.071	0.068	0.072	0.072	0.071	0.071	0.070	0.070
1.25E+00	0.063	0.062	0.062	0.061	0.060	0.059	0.060	0.058	0.064	0.064	0.064	0.064	0.063	0.062
1.50E+00	0.057	0.056	0.056	0.055	0.054	0.053	0.053	0.052	0.059	0.058	0.058	0.058	0.057	0.057
2.00E+00	0.049	0.049	0.048	0.048	0.047	0.046	0.047	0.046	0.050	0.050	0.050	0.050	0.049	0.049
3.00E+00	0.041	0.041	0.041	0.041	0.042	0.041	0.042	0.041	0.040	0.040	0.040	0.040	0.039	0.039
4.00E+00	0.037	0.036	0.038	0.038	0.040	0.040	0.040	0.040	0.034	0.034	0.034	0.034	0.033	0.033
5.00E+00	0.034	0.034	0.037	0.036	0.040	0.039	0.040	0.040	0.030	0.030	0.030	0.030	0.029	0.029
6.00E+00	0.032	0.032	0.036	0.035	0.040	0.039	0.041	0.040	0.027	0.027	0.027	0.027	0.027	0.026
8.00E+00	0.031	0.030	0.035	0.034	0.041	0.040	0.042	0.041	0.024	0.023	0.023	0.023	0.023	0.023
1.00E+01	0.030	0.029	0.036	0.035	0.043	0.042	0.044	0.043	0.021	0.021	0.021	0.021	0.021	0.021
1.50E+01	0.030	0.029	0.037	0.037	0.048	0.046	0.049	0.048	0.018	0.018	0.018	0.018	0.018	0.017
2.00E+01	0.030	0.030	0.039	0.039	0.051	0.051	0.053	0.052	0.016	0.016	0.016	0.016	0.016	0.016

The variation of mass attenuation coefficient of PbBPE samples versus incident photon energy is shown in Fig 2. It shows that for material P202, P204, P206 and PB202, multiple peaks of mass attenuation coefficient in the low energy region were observed because of the K, L and M absorption edges of Pb. The μ_m decreases with the photon energy increasing at first but increases when the energy

exceed 3MeV. For B201, B202 and B203, the mass attenuation coefficient decreases rapidly with the increase of the photon energy in the low energy region, whereas slowly in the high energy region. The P202, P204, P206 and PB202 has higher μ_m than others when the photon energy is below 0.6MeV or over 3MeV, while it is approximately equal at the photon energy range from 0.6MeV to 3MeV.

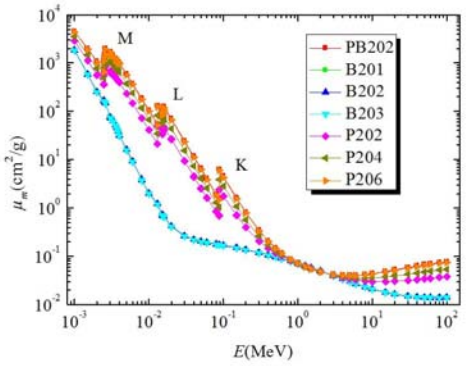

Fig. 2 Variation of mass attenuation coefficient of PbBPE samples versus incident photon energy

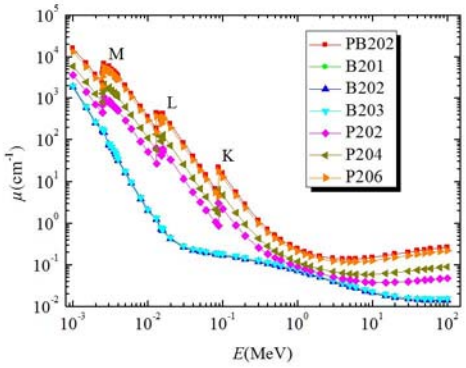

Fig. 3 Variation of linear attenuation coefficient of PbBPE samples versus incident photon energy

3.2. Linear attenuation coefficient (μ)

Fig 3 shows the variation of linear attenuation coefficient of PbBPE samples versus incident photon energy. It is observed that the variation of$\mu$is similar to μ_m but the gaps of each graph becomes larger by a factor according to the density of each material, especially when the photon energy range is between 0.6MeV and 3MeV. The PB202 sample has the highest linear attenuation coefficient over all the photon energy range due to its high density and the high containment of element Pb. The linear attenuation coefficients of B201, B202 and B203 are basically equal over all the photon energy range.

3.3. Mean free path (MFP)

As shown in Fig 4, The mean free path increases rapidly with the increase of the photon energy in the low energy region, whereas slowly in the high energy region for B201, B202 or B203. For the P202, P204, P206 and PB202, multiple peaks of *MFP* in the low energy region were observed because of the K, L and M absorption edges of Pb, and the *MFP* decreases when the photon energy exceed 3MeV. Mathematically *MFP* is inversely proportional to μ hence the PB202 sample has the lowest *MFP* overl the entire photon energy range. So PB202 is better than other samples for photon attenuation.

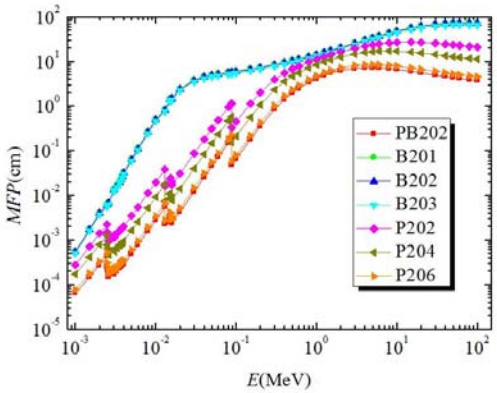

Fig. 4 Variation of mean free path of PbBPE samples versus incident photon energy

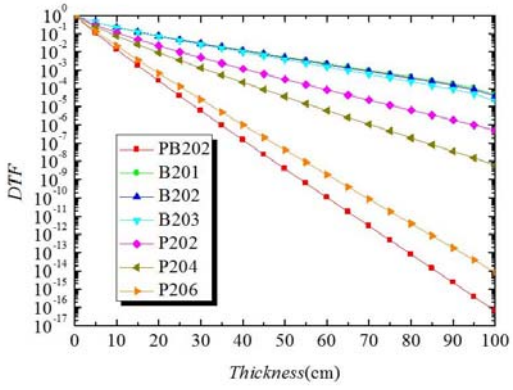

Fig. 5 Variation of *DTF* versus shielding thickness for Cesium-137 (0.662MeV) source

3.4. Dose transmission factor (DTF)

The variation of dose transmission factor of PbBPE samples versus shielding thickness for Cesium-137 (0.662MeV), Cobalt-60 (1.1732MeV) and Cobalt-60 (1.3325MeV) source are shown in Figs. 5-7. It can be seen that the source energy has a great impact on *DTF*, for the Cesium-137 (0.662MeV) source which shown in Fig. 5 the $DTF \approx 10^{-16}$ when the shielding thickness of PB202 is 100cm, whereas these values are 10^{-10} and 10^{-9} for the Cobalt-60 (1.1732MeV) and Cobalt-60 (1.3325MeV) source as shown in Fig. 6 and 7. These figures show that the variation law of dose transmission factor for these sources are similar, but they drop all according to the following order: PB202>P206>P204>P202>B203>B202>B201.

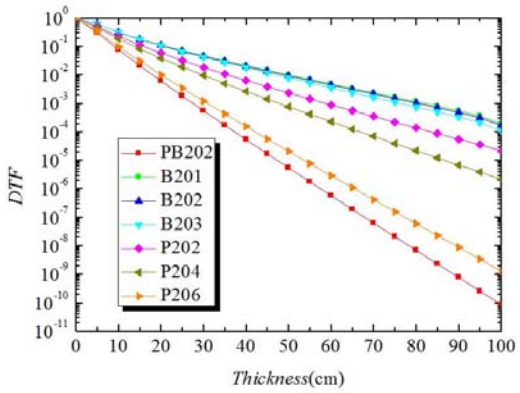

Fig. 6 Variation of *DTF* versus shielding thickness for Cobalt-60 (1.1732MeV) source

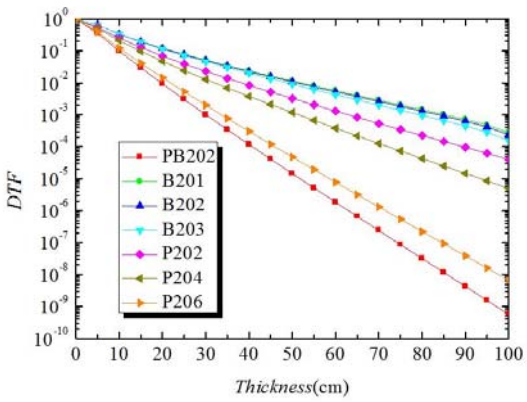

Fig. 7 Variation of *DTF* versus shielding thickness for Cobalt-60 (1.3325MeV) source

4. Conclusion

In this study, the mass attenuation coefficient (μ_m), linear attenuation coefficient (μ), mean free path (*MFP*) as well as dose transmission factor (*DTF*) of the high effective shielding material Lead-Boron Polyethyene are simulated by MCNP code. It can be concluded that the photon attenuation coefficients of any shielding material depends on the photon energy, material density and atomic composition. To select an appropriate shielding material, all this parameters should be considered thoroughly. For source Cesium-137 (0.662MeV), Cobalt-60 (1.1732MeV) and Cobalt-60 (1.3325MeV), PB202 is a good shielding material among the seven PbBPE samples. The results of this paper can provide some reference for the future use of the Lead-Boron Polyethyene. We can also conclude that the simulation way based on MCNP to obtain photon attenuation coefficients can be used to simulate other types of shielding materials.

References

[1] Akio, Y., Kiyoshi, S., 1994. Shielding design to obtain compact marine reactor. J. Nucl. Sci. Technol. 31, 510-520.

[2] Lv, J., Chen, J., 1994. High effective shielding material lead-boron polyethylene. Nucl. Power Eng. 15, 370-374.

[3] Shin, J.W., Lee, J.W., Yu, S., Baek, B.K., Hong, J.P., Seo, Y., Kim, W.N., Hong, S.M., Koo, C. M., 2014. Polyethylene/boron-containing composites for radiation shielding. Thermochim. Acta 585, 5-9.

[4] Elmahroug, Y., Tellili, B., Souga, C., 2015. Determination of total mass attenuation coefficients, effective atomic numbers and electron densities for different shielding materials. Ann. Nucl. Energy 75, 268-274.

[5] Biswas, R., Sahadath, H., Mollah, A.S., Huq, M.F., 2016. Calculation of gamma-ray attenuation parameters for locally developed shielding material: Polyboron. J. Radiat. Res. Appl. Sci. 9, 26-34.

[6] Tarim, U.A., Gurler, O.，Ozmutlu, E.N., Yalcin, S., 2013. Monte Carlo calculations for

gamma-ray mass attenuation coefficients of some soil samples. Ann. Nucl. Energy 58, 198-201.

[7] Oto, B., Gür, A., Kaçal, M.R., Dogan, B., Arasoglu, A., 2013. Photon attenuation properties of some concretes containing barite and colemanite in different rates. Ann. Nucl. Energy 51, 120-124.

[8] Adem, U., Faruk, D., 2013. Determination of mass attenuation coefficients, effective atomic numbers and effective electron numbers for heavy-weight and normal-weight concretes. Appl. Radiat. Isot. 80, 73-77.

[9] Singh, V.P., Ali, A.M., Badiger, N.M., El-Khayatt, A.M., 2013. Monte Carlo simulation of gamma ray shielding parameters of concretes. Nucl. Eng. Des. 265, 1077-1071.

[10] Sharifi, S., Bagheri, R., Shirmardi, S.P., 2013. Comparison of shielding properties for ordinary, barite, serpentine and steel–magnetite concretes using MCNP-4C code and available experimental results. Ann. Nucl. Energy 53, 529-534.

[11] Tellili, B., Elmahroug, Y., Souga, C., 2014. Determination of mass attenuation coefficient, effective atomic number and effective electron density for tungsten alloys. Int. J. Nucl. Energy Sci. Technol. 8, 238-248.

[12] El-Khayatt, A.M., Ali, A.M., Singh, V.P., 2014. Photon attenuation coefficients of Heavy-Met al Oxide glasses by MCNP code, XCOM program and experimental data: A comparison study. Nucl. Instrum. Methods Phys. Res. Sect. A 735, 207-212.